Numerical Investigation of Heat Transfer Enhancement of a Water/Ethylene Glycol Mixture with Al2O3-TiO2 Nanoparticles

Fahad Alshehri, Jaydeep Goraniya and Madeleine L Combrinck

Northumbria Universit, Newcastle-upon-Tyne, NE18ST, United Kingdom

Abstract

This paper presents a numerical study of a four-component hybrid nanofluid consisting of binary nanoparticles, Al_2O_3 and TiO_2, dispersed into a double base fluid mixture of water and ethylene glycol. The nanofluid were modelled as a single phase fluid with volume concentrations of 2.5% Al2O3-1.5% TiO2 and 5% Al2O3-3% TiO2 respectively. The nanoparticles are suspended in a double base fluid of water and ethylene glycol mixture with a 70:30 volume ratio. The simulations were conducted for turbulenct flow through a pipe at working temperatures of 293 K and varying Reynolds numbers (7800-2000). Constant heat flux of 129983 W/m^2 heat flux was applied to the pipe wall. The thermal conductivity was enhanced by 24 % and 11% at concentrations of 5-3% and 2.5-1.5%, respectively. While, viscosity of hybrid nanofluids was rising up to 70% and 67% at the same concentration. The avarage heat transfer coefficient of Al2O3-TiO2 hybrid nanofluids were enhanced with increase of temperature and volume concentration. It was noted that the maximum heat transfer enhancement is 52% higher than the base fluid for a volume concentration of 5-3%. There is a slight increase in the friction factor of Al2O3-TiO2 hybrid nanofluids with higher volume concentration.

Keywords: Hybrid nano fluid, single phase approximation, viscosity, thermal conductivity, performance factor

1. Introduction

The development of cooling systems to achieve optimal performance is a key research area in sustainable engineering. Cooling efficiency is a consideration in numerous applications, such as large power transformers, engines and electronic products. Automotive engines rely on cooling systems to remove excessive heat and prevent damage to engine parts as well as other adjacent systems. Temperature control with a cooling system ensures sustained operation and maintenance of such systems. Heat management conventionally uses fluids such as oil, ethylene glycol and water. Heat transfer ability is enhanced using a number of methods including pure forced convection of fluids, extended surface technique and employment of mini/micro channel heat exchange systems. The ability of these methods to manage with higher thermal fluxes is limited. Consequently, there is a rise in demand for development of other heat transfer enhancement techniques. Thermal conductivity of solids materials is generally greater than liquids, therefore suspending solid particles in a fluids will greatly enhance the thermal characteristics (Ebrahimi et al., 2010).

Masuda et al., (1993) studied the thermophysical characteristics of ultra-fine particles dispersed in liquids. This included quantifying the viscosity and heat conductivity of modified heat-transfer fluids at small volume concentrations. The name nanofluids were originally employed by Choi (1995) when referring to suspended nanoparticles. A nanofluid can be described as a stable, homogeneous suspension containing nanoparticles smaller than 100nm on average (Choi, 1995) with the aim of heat transfer ability of the base liquid.

Hybrid nanofluid involves the dispersion of two or more nanoparticles in a heat transfer liquid (Akilu et al., 2016). The thermophysical properties of hybrid nanofluids have been investigated in research studies (Madhesh and Kalaiselvam, 2014; Bahrami et al., 2016). Research reviews were conducted by Hamzah et al. (2017) and Sidik et al. (2017). Their respective studies showed a need for further research into the thermophysical properties of hybrid nanofluids to broaden understanding of physical behaviour.

This paper numerically evaluate the thermal performance of hybrid nanofluid consisting of Alumina (Al_2O_3) and

* Corresponding author. Madeleine L Combrinck Tel.: +44 0191 299 4549; e-mail: madeleine.combrinck@northumbria.ac.uk

Titania (TiO_2) with 2.5% – 5% and 1.5% – 3% concentrations, respectively. This is dispersed in a double base mixture of ethylene glycol (EG, 30% by volume) and water (70% by volume).

Numerous studies have investigated the heat transfer behaviour of hybrid nanoparticles, including aluminium, copper, silicon, titanium, and their oxides dispersed in liquids, such as water or ethylene glycol (Deepak Selvakumar and Dhinakaran, 2016; Kumar and Sonawane, 2016). Studies investigating hybrid nanoparticles dispersed in a double base fluid mixture, i.e., four constituents, are rare. The selection of a four-component hybrid nanofluid consisting of TiO_2 and Al_2O_3 nanoparticles, and ethylene glycol and water as a double base fluid mixture, are rationalised as follow:

i. the selected nanoparticles, aluminium and titanium, are inexpensive and readily available,
ii. titanium is considered eco-friendly, and
iii. the base fluid mixture of ethylene glycol and water has high boiling and low freezing points as compared to pure water (ASHRAE, 1979).

2. Thermal Properties of Hybrid Nano Fluids

The two properties of hybrid nanofluids, namely viscosity and thermal conductivity, have been the focus of researchers in recent years. The studied aimed at developing nanofluids with lower viscosity and improved heat transfer potential to demonstrate long-term stability.

2.1 Thermal Conductivity

The heat transfer behaviour of Al2O3-Cu/water hybrid nanofluids was investigated by Suresh *et al.*, (2011). The researchers employed nanoparticles with average particle size of 17nm and volume concentration of 0.1 – 2.0% at 32°C temperature. The study revealed a positive association between volume concentration of nanoparticles and thermal conductivity of Al_2O_3-Cu/water hybrid nanofluids. The highest thermal conductivity performance recorded at nanoparticles volume concentration of 2.0% was estimated to be 12.11%. The enhanced thermal conductivity of the hybrid nanofluids under investigation can be attributed to the functionalized Cu and Al2O3 nanoparticles.

Esfe *et al.*, (2015) evaluated thermal conductivity of ethylene glycol and water (40:60) mixture based hybrid nanofluids containing Cu and TiO_2 nanoparticles. Various temperatures between 30°C and 60°C were analysed, and different nanoparticles volume concentrations ranging from 0.1% to 2.0 % to estimate thermal conductivity of hybrid nanofluids. The findings revealed that increase in temperature as well as nanoparticles volume concentration had a positive correlation with thermal conductivity. The maximum relative thermal conductivity measured was 1.43 at 60°C temperature and 2.0% volume concentration.

Harandi *et al.*, (2016) carried out assessment of the influence of volume concentration and temperature on thermal conductivity performance of ethylene glycol and water-based hybrid nanofluids containing Fe_3O_4 and f-MWCNTs nanoparticles. They used temperatures ranging from 25°C to 50°C, and nanoparticles volume fraction ranging between 0.1% and 2.3% for the experimentation. The study found that an increment in temperature and solid volume concentration leads to enhancement of thermal conductivity. The findings also demonstrated that variation of nanoparticles volume concentration with thermal conductivity ratio was greater at higher temperature as compared to that at lower temperature values. Moreover, higher volume concentrations of nanoparticles revealed very distinct effects of temperature on thermal conductivity behaviour. The experiment required a 2.3% volume concentration and 50°C temperature to produce highest thermal conductivity enhancement of about 30%. The findings of the study also suggest that thermal conductivity performance of nanofluids was lower as compared to that of the hybrid nanofluids.

2.2 Viscosity

The amount of research literature involving the viscosity of nanofluids was comparatively scarce. However, since viscosity can affect the heat transfer and flow behaviour, its impacts are considered as significant as that of thermal conductivity.

Ho *et al.*, (2010) analysed the dynamic viscosity of hybrid water based mixture containing Al_2O_3 nanoparticles and MEPCM particles of different volume fractions at 30°C. The authors found that effective dynamic viscosity of hybrid nanofluids as enhanced with addition of nanoparticles to the PCM suspension.

The viscosity of Al2O3-Cu containing water-based hybrid nanofluids with different volume fractions ranging between 0.1 – 2.0% was evaluated by Suresh *et al.*, (2011) at temperature of 32°C. The authors observed that hybrid nanofluids depicted a Newtonian behaviour since dependence of viscosity on shear rate was not found. The

findings revealed a positive association between volume fraction and viscosity. The comparison between viscosities of Al_2O_3-Cu/water based hybrid nanofluids and Al_2O_3-water based nanofluids demonstrated that the variation between Al_2O_3-Cu/water based hybrid nanofluid and Al_2O_3/water nanofluid was significant at higher nanoparticle volume fractions while lower at small nanoparticle volume fractions. The observed enhancement in relative viscosity of hybrid nanofluid can be attributed to the increase in the hydrodynamic size of nanoparticles because of surface adsorption and agglomeration, which leads to an increase in nanoparticle volume concentration.

The viscosity of SiO2 and MWCNTs containing nanofluids and SiO2-MWCNTs/water based hybrid nanofluids prepared in 80:20 and 50:50 ratios was assessed by Baghbanzadeh *et al.*, (2014). Temperatures ranging from 10℃ to 40℃ and three nanoparticle volume fractions of 0.1%, 0.5% and 1.0% were analysed. The study found that kinematic viscosity is enhanced with increase in nanoparticle volume concentration but decreases with rise in temperature. The observed enhancement in viscosity of the hybrid nanofluids can be attributed to higher concentration of nanoparticles achieved because of cluster formation and internal viscous stress. Furthermore, the weakening of the intermolecular attractions because of rise in temperature can also lead to lower viscosity. The enhanced viscosity of the hybrid nanofluid as a result of higher nanoparticle volume concentrations was inclined more towards the Silica nanofluid viscosity and was found to be lower than the viscosity of MWCNTs nanofluid.

Esfe *et al.*, (2015) evaluated the dynamic viscosity of water based hybrid nanofluids dispersed with MgO and Ag nanoparticles at volume concentrations ranging between 0.5% and 2.0%. The findings revealed that higher volume concentration of nanoparticles lead to enhanced dynamic viscosity. The study measured a ratio of 1.38 between the base fluid viscosity and the viscosity of hybrid nanofluid, referred to as dynamic viscosity ratio, at a volume concentration of 2.0%.

Bahrami *et al.*, (2016) attempted to analyse the influence of nanoparticle volume concentration and temperature on viscosity of ethylene glycol and water (80:20) based hybrid nanofluids containing CuO and Fe nanoparticles. The study employed temperature ranging between 25℃ to 50℃ and 6 nanoparticle volume fractions ranging between 0.05% and 1.5%. A low viscosity was observed at low temperatures, while enhanced viscosity at higher nanoparticle volume concentrations. Moreover, lower viscosity was measured because of the increase in nanoparticle volume concentration coupled with higher shear rate. The van der Waals forces existing between the nanoparticles cause agglomeration, which leads to the enhancement of hybrid nanofluid viscosity. Furthermore, the researchers observed power law index closer to one, which suggests that lower nanoparticle volume concentrations led to the formation of Newtonian behaviour. The Newtonian behaviour of hybrid nanofluids can change into non-Newtonian behaviour at higher nanoparticle volume concentrations.

3. Recent Studies

To employ enhanced thermal conductivity of hybrid nanofluids in various applications, the measurement of pressure drop, friction factor and heat transfer behaviour of these fluids becomes imperative. Several studies have thus attempted to determine pressure drop and thermal conductivity behaviour of hybrid nanofluids both experimentally and numerically.

3.1 Experimental Studies

Hussein (2017) carried out experiments using a double pipe heat exchanger to measure friction factor and Nusselt number for ethylene glycol based Aluminium Nitride nanoparticles having volume fractions ranging from 1% to 4%. The study found significant positive correlation between nanoparticle volume concentration and friction factor as well as Nusselt number. An enhancement of about 35% was observed in Nusselt number, while an increase of 12.5% was recorded for values of friction factor. The authors concluded that enhanced hydrodynamic flow and heat transfer performance of ethylene glycol based Aluminium Nitride hybrid nanoparticles makes them highly suitable for industrial use.

A study by Suresh *et al.*, (2012) aimed to assess the pressure drop and thermal convection in a laminar pipe flow by employing Al_2O_3–Cu/water based hybrid nanofluid with nanoparticle volume concentration of 0.1%. The Al2O3–Cu hybrid nanoparticles depicted better thermal conductivity performance as compared to the pure water model. Moreover, a comparison of Al_2O_3/water based nanofluids and Al_2O_3–Cu/water based hybrid nanofluids revealed that the latter produced additional penalty in relation to pumping power.

Another investigation by Suresh *et al.*, (2014) attempted to assess the pressure drop and heat transfer behaviour in a turbulent pipe flow by employing water based hybrid nanofluid containing Cu and Al_2O_3 nanoparticles with volume concentration of about 0.1%. In comparison with pure water, the heat transfer performance of hybrid nanofluid was found to be enhanced by about 8.02%. It was

* Corresponding author. Madeleine L Combrinck Tel.: +44 0191 299 4549; e-mail: madeleine.combrinck@northumbria.ac.uk

also observed that the Al2O3/water nanofluid had a lower friction factor as compared to Al_2O_3-Cu/water hybrid nanofluid at similar conditions for nanoparticle volume concentration.

Ho, Chen and Yan, (2014) investigated thermal convection in a mini-channel heat sink (Mini-CHS) flow by using microencapsulated phase change material (MEPCM) particles and Al_2O_3/water based nanofluid. About ten rectangular mini-channels are combined together to form a copper heat sink. The study revealed that heat sink flow rate affect the heat transfer performance of PCM suspension and Al2O3/water based nanofluid to a significant extent. Moreover, higher volume concentration of solids leads to a significant increase in values of friction factor.

Sundar, Singh and Sousa, (2014) assessed the friction factor and convection coefficient in a turbulent pipe flow by using water based hybrid nanofluids dispersed with Fe3O4 nanoparticles and MWCNTs with nanoparticle volume concentrations ranging from 0.1% to 0.3%. The condition of a constant boundary temperature was applied. The researchers observed an increase in friction factor and Nusselt number at higher nanoparticle volume concentration. The higher heat transfer performance of MWCNT–Fe3O4 based hybrid nanofluids can be attributed to various factors, including enhanced surface area and Brownian motion of particles.

A study by Madhesh, Parameshwaran and Kalaiselvam, (2014) employed a tubular counter flow heat exchanger to analyse rheological behaviour and heat transfer performance of Cu–TiO2 based hybrid nanofluids with nanoparticles volume fractions ranging between 0.1% and 2.0%. The scholars observed enhancement in Nusselt number and convection coefficient at 1% volume concentration. The pressure drop and friction factor values at volume concentration of 2% indicated additional penalty in terms of pumping power. The study showed that enhanced heat transfer performance was due to Cu–TiO2 nanoparticles and lower thermal resistance faced during the flow.

3.2 Numerical Studies

Saha and Paul (2014) conducted experiments to numerically evaluate the heat transfer performance and flow behaviour of water based nanofluids containing TiO_2 and Al_2O_3 nanoparticles subjected to turbulent tube flow. The study found that in contrast to the base fluid, nanofluids exhibited a higher shear stress ratio and average Nusselt number. The nanoparticle volume concentration of 6% and particle size of 10nm depicted a higher thermal performance factor for any size of nanoparticles as well as Reynolds number. Moreover, additional pump power penalty was prevented because of the insignificant impact of nanofluid friction factor relative to the base fluid.

A study conducted by Labib *et al.*, (2013) investigated the influence of Reynolds number and nanoparticle volume concentration on heat transfer performance of water based hybrid nanofluids containing CNTs and Al_2O_3 nanoparticles subjected to laminar pipe flow. The simulations based on a two phase mixture model were carried out by employing the CFD commercial code. A laminar, steady state flow was taken into consideration. It was found that the water based mixture dispersed with a combination of CNTs and Al_2O_3 nanoparticles led to significant enhancement of heat transfer performance. Moreover, the study observed that higher nanoparticle volume concentration and friction factor of hybrid nanofluid was associated with enhanced convective coefficient.

Moghadassi, Ghomi and Parvizian, (2015) evaluated the forced convective heat transfer in laminar pipe flow by using water based hybrid nanofluids containing Cu and Al_2O_3 nanoparticles with average size 15nm and volume concentration of 0.1%. The study made use of both single phase and two phase models for carrying out simulations. The pressure-velocity coupling was addressed by employing the SIMPLE algorithm. The findings revealed enhanced convective coefficient for hybrid nanofluid. In comparison to pure water and Al2O3/water based nanofluids, about 13.46% and 4.73% average enhancement in Nusselt number was observed for Al2O3-Cu/water based hybrid nanofluids, respectively, in the single phase model. However, the Nusselt number depicted a 4% increase as compared to the Al_2O_3/water based nanofluids in the two phase model. The two phase model was found to be a better predictor of the experimental results as compared to the single phase model.

The forced convective heat transfer in turbulent pipe flow by employing water based hybrid nanofluids containing Cu and Al_2O_3 nanoparticles with volume concentrations ranging between 0% and 2% were studied by Takabi and Shokouhmand, (2015). The results revealed that although heat transfer performance of hybrid nanofluids was significantly enhanced, pressure drop and friction factor were severely affected.

Minea (2017b, 2017a) employed a 3D tube model to compare and assess heat transfer behaviour of various hybrid nanofluids. Simulations based on single phase model were carried out by employing the CFD commercial code. A steady state, turbulent flow was taken into consideration for this study and the k- ϵ turbulent model was employed. Numerical analysis revealed a higher

Nusselt number of 241% for hybrid nanofluids (Al2O3–SiO2) and 257% enhancement of convective coefficient along with a significant increase in viscosity.

4. Methodology

4.1 Case Description

The research literature contains two types of studies which depict hydrodynamic and heat transfer performance through quantitative modelling. The first group asserts that since the relative velocity between the liquid and solid components is equal to zero, the fluids are in thermal equilibrium with the suspended solid particles and the two components move along each other with an equal velocity. Others, such as Xuan and Li (2000), contend that there is only a single phase fluid as the very minute particle size leads to fluidisation of the solid particles.

Based on the single phase simulations, this study has shown CFD models which employ surface tube with uniform temperature for fully developed turbulent flows. There is thermal equilibrium between the solid particles and the fluid phase and they are moving as a single phase with equal velocity. In addition, the heat transfer performance of hybrid nanofluids (HyNf) and the turbulent flow in a channel with uniform boundary temperature are presented using a two dimensional axisymmetric simulation. The geometry of the circular pipe with a diameter (D) of 0.014m and length (L) of 1.75m is illustrated in Figure 1. The horizontal plane (along the x–axis) will theoretically be axisymmetric with respect to the heat fields and turbulent flow.

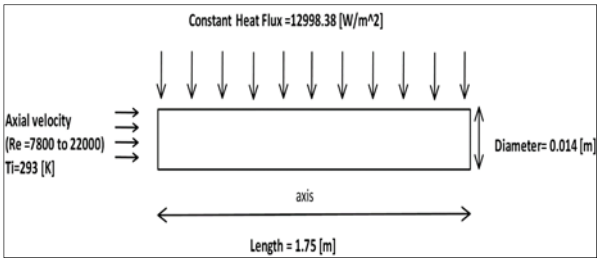

Figure 1: Schematic diagram of the current geometry

The experimental system used by Suresh *et al.*, (2011) forms the basis for the numerical analysis performed here. The axial velocity of the inflowing fluid remains uniform with a steady temperature of 300 K. The Reynolds number widely fluctuated, ranging between 7800 and 22000.

4.2 Thermal Property Models for HyNf

In order to manage the potential issues associated with production and energy conservation, it is imperative to envisage the thermophysical and heat transfer characteristics of nanofluids. Although several research studies have attempted to evaluate the thermal behaviour of nanofluids, only a few studies have investigated the overall thermophysical properties of respective HyNf comprehensively. A majority of the studies focus on evaluation of certain variables, such as thermal conductivity and viscosity, and provide with a description of the preparation technique. However, these studies are quite limited in scope and fail to provide a comprehensive insight into the heating behaviour of nanofluids.

Al_2O_3 and TiO_2 nanoparticles with 2.5% – 5% and 1.5% – 3% concentrations, respectively, were dispersed in a mixture of ethylene glycol (EG, 30% by volume) and water (70% by volume) for preparation of HyNf in this study. The thermophysical properties of HyNf constituents, such as base fluids and oxide nanoparticles, are presented in Table 1.

Table 1: Thermal properties of HyNf components at T = 293 K (Minea, 2017b).

	Density [kg/m³]	Specific heat [W/kg K]	Viscosity [kg/m s]	Thermal conductivity [W/m K]
Water	996.5	4181	0.001	0.613
Ethylene glycol	1111.4	2415	0.0157	0.252
Al_2O_3	3970	765	-	40
TiO_2	4175	692	-	8.4

The MATLAB Curve Fitting Toolbox was employed to measure the thermophysical properties, such as density, specific heat capacity, viscosity and thermal conductivity, of the base fluid using data for ethylene glycol solution (30% volume) obtained from ASHRAE Handbook (1979). To compute the values for properties of base fluid mixture, correlations applicable over $261 \leq T\ (K) \leq 394.26$ are given below.

$$\rho_f = -2.425 \times 10^{-3}\, T^2 + 1.0453\, T + 948.5 \qquad R^2 = 1 \tag{1}$$

$$\mu_f = 1.391 \times 10^4 \exp(-0.05738\ T) + 0.1104 \exp(-0.01466\ T); \qquad R^2 = 0.99 \tag{2}$$

* Corresponding author. Madeleine L Combrinck Tel.: +44 0191 299 4549; e-mail: madeleine.combrinck@northumbria.ac.uk

$$k_f = 2.574 \times 10^{-9}\, T^3 - 7.545 \times 10^{-6}\, T^2 + 4.752 \times 10^{-3}\, T - 0.3638; \quad R^2 = 0.99 \tag{3}$$

$$C_{p_f} = 5 \times 10^{-5}\, T^2 + 2.8\, T + 2820.4; \quad R^2 = 0.99 \tag{4}$$

Pak and Cho (1998) used a number of equations for measuring density and specific heat capacity of HyNf. These equations are regarded as classical associations between HyNf constituents and have been widely employed in several studies. The mean values of properties were computed according to the volume proportion of the nanoparticles. The properties, such as specific heat capacity and density, for phase change material added to water and Al_2O_3 nanoparticles were measured using equations (5) and (6) employed by Ho *et al.*, (2010).

$$\rho_{nf} = \varphi_{np1}\, \rho_{np1} + \varphi_{np2}\, \rho_{np2} + (1 - \varphi_{np1} - \varphi_{np2})\, \rho_f \tag{5}$$

$$\rho_{nf} C_{p_{nf}} = \varphi_{np1} \rho_{np1} C_{p_{np1}} + \varphi_{np2} \rho_{np2} C_{p_{np2}} + (1 - \varphi_{np1} - \varphi_{np2}) \rho_f C_{p_f} \tag{6}$$

The measurements for mixture comprised of three constituents (where the double-based fluid is incorporated as a single liquid mixture k_f) can be treated using various approaches. A convenient and direct technique is the modification of an equation intended for two elements into an equation for three elements. The equation for three elements employed in this study is a generalised form of Maxwell's equation developed in a similar way by Brailsford and Major (1964).

$$k_{eff} = k_f \left[1 + \frac{3\varphi_1 \frac{k_1 - k_f}{2k_f + k_1} + 3\varphi_2 \frac{k_2 - k_f}{2k_f + k_2}}{(1 - \varphi_1 - \varphi_2) + 3\varphi_1 \frac{k_f}{2k_f + k_1} + 3\varphi_2 \frac{k_f}{2k_f + k_2}} \right] \tag{7}$$

To determine viscosity, estimation models were employed. The Batchelor (1977) model, which has been commonly employed in the research literature, was used first for a theoretical estimation.

$$\frac{\mu_{eff}}{\mu_f} = 1 + 2.5\varphi + 6.2\varphi^2 \tag{8}$$

The model developed by Pak and Cho (1998) for estimation of effective viscosity of Al_2O_3–water nanofluids was employed in the present study.

$$\frac{\mu_{eff}}{\mu_f} = 1 + 39.11\varphi_{Al_2O_3} + 533.9\varphi^2{}_{Al_2O_3} \tag{9}$$

The estimation model developed by Buongiorno (2006) was employed for TiO_2–water based nanofluids.

$$\frac{\mu_{eff}}{\mu_f} = 1 + 5.45\varphi_{TiO_3} + 108.2\varphi^2{}_{TiO_3} \tag{10}$$

Calculation of the mean value for equations (9) and (10) will present the overall effective viscosity.

The local Nu and local h of HyNf are determined form following equations:

$$Nu_{(x)} = \frac{h_{(x)} D}{k} \tag{11}$$

$$h_{(x)} = \frac{\dot{q}_s}{T_w - T_m(x)} \tag{12}$$

$T_m(x)$ is the mean temperature of a fluid for constant and uniform heat flux $\dot{q}_s$ and $\dot{m}$ is the mass flow rate. $T_w(x)$ is the wall temperature.

$$T_m(x) = T_{m,i} + \frac{\dot{q}_s \pi D}{\dot{m} C_p} x \tag{13}$$

$$T_w(x) = \frac{\dot{q}_s}{h_{(x)}} + T_m(x) \tag{14}$$

The average Nu is then defined as:

$$\overline{Nu} = \frac{1}{L} \int_0^L Nu\,(x) dx \tag{15}$$

Darcy friction factor for turbulent flows in a pipe is determined by:

$$f = \frac{2 D_h \Delta p}{\rho L v_m^2} \tag{16}$$

2.3 Governing Equations

The following assumptions are made with regards to the fluid:

i. The HyNf is incompressible, turbulent and Newtonian fluid.

ii. The horizontal placement of the pipe makes the Boussinesq approximation inconsequential.
iii. There is a thermal equilibrium between solid nanoparticles and the fluid phase and it moves with an equal velocity.
iv. The shape and size of nanoparticles is the same and globular.
v. The impacts of radiation and viscous dissipation can be neglected.

If the assumption about base fluid being a Newtonian fluid is true, it follows that the nanofluid having lower 10% volume fraction with water as compared to the base fluid would also be considered a Newtonian fluid. According to Kakaç and Pramuanjaroenkij (2016), it has been observed that nanofluids have comparatively lower than 10% volume fraction.
Considering the aforementioned assumption, following are the transient-state governing equations for single-phase simulation of heat transfer and HyNf flow.

Continuity equation:

$$\frac{\partial \rho}{\partial t} + \nabla . \bar{v} = 0 \tag{17}$$

Momentum equation:

$$\frac{\partial \rho \bar{v}}{\partial t} + div(\rho \bar{v}\bar{v}) = -\nabla(P) + \mu \nabla^2 \bar{v} - div(\rho \overline{u'}\overline{u'}) \tag{18}$$

Energy equation:

$$\frac{\partial \rho E}{\partial t} + div(\rho \bar{v} c_p \bar{T}) = div(k\, \nabla d\bar{T} - \rho c_p \overline{u'}\overline{t'}) \tag{19}$$

2.4 Turbulent modelling

The governing equations of the fluid flow closed by employing approximate simulation or experimental findings that can depict the heat flux measurements and turbulent stresses of the associated physical occurrence. This study employed the realizable $\kappa - \epsilon$ turbulent model developed by Shih *et al.*, (1995) which is different from standard $k - \epsilon$ model because of two reasons. An alternate formulation for the turbulent viscosity has been incorporated into the realizable $\kappa - \epsilon$ turbulent model on the one hand, while the precise expression for the transport of the mean-square vorticity variation has facilitated creation of a new transport expression for dissipation rate on the other Shih *et al.*, (1995). In order to assess the fluctuations in completely developed turbulent kinetic energy, three different models of turbulence, such as the standard $\kappa - \epsilon$ turbulent model, the realizable $\kappa - \epsilon$ turbulent model and the RNG $\kappa - \epsilon$ turbulent model, were evaluated by Saha and Paul (2014). The scholars compared and contrasted the results with the empirical findings of Fan, Lakshminarayana and Barnett (1993), Schildknecht, Miller and Meier (1979), and Launder B.E. and Sharama (1974) revealed that the realizable $\kappa - \epsilon$ turbulent model demonstrated a superior performance as compared to the other two models.

The dissipation rate of turbulent kinetic energy (ϵ) and turbulent kinetic energy employed in the realizable $\kappa - \epsilon$ turbulent model is expressed as;

$$div(\rho \kappa \vec{v}) = div\left\{\left(\mu + \frac{\mu_t}{\sigma_k}\right) grad\ \kappa\right\} + G_\kappa - \rho\epsilon \tag{20}$$

$$div(\rho \epsilon \vec{v}) = div\left\{\left(\mu + \frac{\mu_t}{\sigma_\epsilon}\right) grad\ \epsilon\right\} + \rho C_1 S_\epsilon - \rho C_2 \frac{\epsilon^2}{\kappa + \sqrt{\nu\epsilon}} \tag{21}$$

where

$$C_1 = max\left[0.43, \frac{\eta}{\eta + 5}\right], \eta = S\frac{\kappa}{\epsilon} \qquad S = \sqrt{2 S_{ij} S_{ij}}. \tag{22}$$

The development of the turbulent kinetic energy because of the average velocity gradients is denoted by G_κ. It is calculated from $\mu_t S^2$, where σ_ϵ and σ_κ are described as the effective Prandtl numbers for the rate of dissipation and turbulent kinetic energy, respectively, and S denotes the modulus of the average rate-of-strain tensor. The μ_t model can be expressed as;

$$\mu_t = \frac{\rho \kappa^2}{\epsilon}\left(A_0 + A_s \frac{\kappa\, U^*}{\epsilon}\right)^{-1} \tag{23}$$

Where A_0 and A_s have values of 4.04 and$\sqrt{6}\, cos\emptyset$, respectively, and are model constants. The value of $\emptyset\ is\ \left(3\ cos^{-1}\sqrt{6}\, W\right)^{-1}$and the angular velocity influences formulations for U^* and W. The model constants given in equations (20) and (21) are $C_2 = 1.9$, $\sigma_\epsilon = 1.2$ and $\sigma_k = 1.0$ (Fluent 6.3 user guide, 2006).

* Corresponding author. Madeleine L Combrinck Tel.: +44 0191 299 4549; e-mail: madeleine.combrinck@northumbria.ac.uk

2.5 Boundary Condition

The two-dimensional test tube system is considered which has been illustrated in Figure 1. Suresh et al. (2011) have described the experimental test tube setup with a length and diameter of 1.75 m and 0.014 m, respectively. A uniform heat flux of 12998.83 W/m^2 was maintained for the tube boundary. The velocity gradients and heat field at the exit point were considered zero, while temperature and velocity were considered uniform at the opening of the tube.

Uniform temperature ($T_i = 293\ K$) and axial velocity (v_i) profiles have been assumed at the opening end of the tube. The intensity of turbulence has also been set constant at 1%. The axial derivatives at the exit of the tube have been assumed to be equal to zero because of the complete development of the conditions. The dissipation rate and turbulent kinetic energy on the tube wall are also considered as zero, while the temperature conditions are assumed to be uniform. A constant gauge pressure ($p_{gauge} = 0$) has been considered at the channel exit and other scalar measurements, such as turbulence and temperature, are derived from the inner flow. It has been assumed that channel is long enough, so that the complete development of temperature fields and flow has occurred by the channel exit.

For near-wall simulation, the enhanced wall treatment technique offers improved functioning Through integration of a two-layer model. The result of enhanced wall treatment would be similar to the traditional simulation if the laminar sublayer can be resolved by a finer near-wall mesh (generally the 1st near-wall node positioned at $Y^+ = 1$), as illustrated in Figure 2. However, the need for large calculations might prove limiting because of the requirement that meshes must be very fine ubiquitously. This is a major condition that is even more significant than obtaining data. Although values of 20 are desirable for accurate inclusion of the boundary layer, the least number of cells required are only 10 (Fluent 6.3 user guide, 2006). To achieve that, inflation was set to 40.

Moreover, it also allows the mesh to sort out viscosity-affected area including the viscous sublayer (Fluent 6.3 user guide, 2006). Because of the aforementioned reasons, enhanced wall treatment was employed in the current study and the Y+ number achieved is 1.26 as shown in Figure 2.

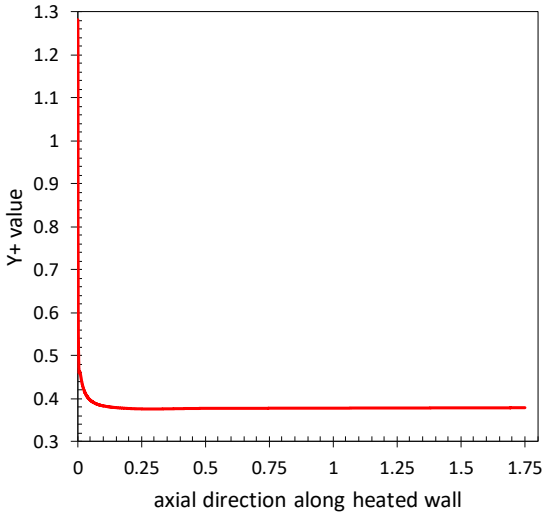

Figure 2: Variation of Y+ along the heated wall at Re 22000 for Al2O3-TiO2 (5-3%)

2.6 CFD Simulation

ANSYS Fluent CFD software package (ver. 18.0) was employed for development of the computational domain. Moreover, the boundary conditions were imposed, and meshing was carried out with the help of ANSYS meshing tool. The Fluent finite volume solver was employed to solve the governing non-liner partial differential equations for turbulence, energy, boundary conditions, momentum and continuity. The finite volume method facilitates the numerical resolution of nonlinear algebraic expressions which have been obtained by conversion of non-linear partial differential equations with second order upwind scheme. In order to obtain a greater accuracy at the cell faces, a Taylor series expansion of the cell-centred solution is performed using the second order upwind scheme. The continuity and momentum equations are used to develop the pressure equation, which can then be solved by employing pressure based solver. A conclusive numerical solution is obtained once all of the equations are solved repetitiously in a specific sequence. All the models in this study considered convergence criteria for the result once the residuals fell below 10^{-12}.

To compute thermophysical characteristics of various HyNf, user-defined functions (UDFs) were used to formulate codes for inclusion of ANSYS-Fluent case file. In order to code the UDF file, C++ programming language was employed.

5. Result and Discussion

5.1 Mesh Independence and Validation Study

Reliable simulation of Computational Fluid Dynamics (CFD) depends on various factors including the mesh resolution and quality. According to recommendations by Casey (2000), the number of cells can be doubled and a comparison carried out on the critical values to prove mesh independence. Three meshes were generated, as shown in Table 2, to ensure that proper validation and verification procedures are observed.

Table 2 Grid independence study - mesh resolution

Model	No of cells
Coarse Mesh	171500
Fine Mesh	344206
Refine Mesh	1662500

Figure 3 shows that all three meshes exhibits similar temperature profiles trends. However, the coarse mesh evidently differs from the refine and fine meshes on two points of the pipe, the centre and close to the pipe's walls.

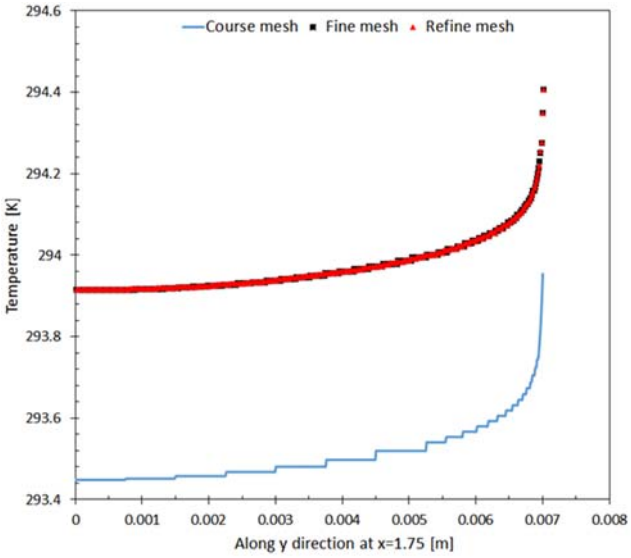

Figure 3: Temperature profile for three different mesh resolutions at x/D =125

The velocity profiles are considered in Figure 4 and both the refine and fine meshes displays similar results.

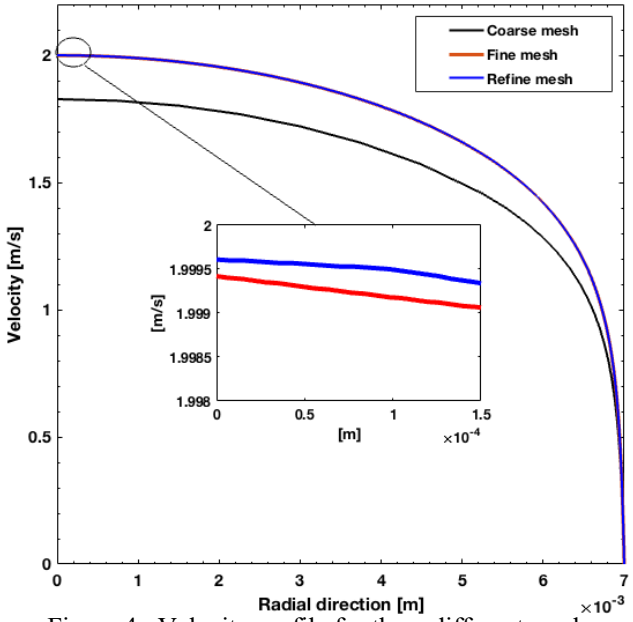

Figure 4: Velocity profile for three different mesh resolutions at x/D =125

Evident from Figures 3 and 4, the fine mesh was selected for the study due to the accuracy that it is more efficient than refine mesh.

Validating of the numerical analysis is done through comparison to analytical analysis of the Nusselt number at $x/D = 125$. The maximum error between numerical and analytical result is 0.114%. Furthermore, traditional expressions of Nu for pure water are compared to these numerical results. Figure 5 below displays the simulation results of turbulent flow under a heat flux that is constant but at different Reynolds. From these results, evidence of an agreement with the Notter-Rouse (1972) equation is seen:

$$Nu = 5 + 0.015Re^{0.856}Pr^{0.347} \tag{24}$$

where

$$Pr = \frac{\mu C_p}{k} \tag{25}$$

* Corresponding author. Madeleine L Combrinck Tel.: +44 0191 299 4549; e-mail: madeleine.combrinck@northumbria.ac.uk

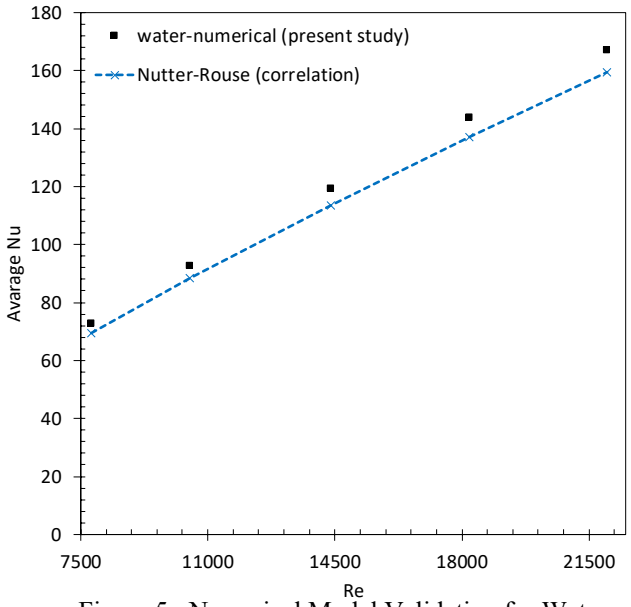

Figure 5: Numerical Model Validation for Water

With respect to the validation of the code, a base fluid made up of 3% Al_2O_3 distilled in water is utilized where Equation (24) is compared with the simulated Nu. The result of the numerically determined Nu was in agreement with the Nutter-Rouse (1972) equation as illustrated in Figure 6.

Similarly, Minea (2017) studied 3% of volume concentration of Al2O3 particles distilled in water base fluid and numerical Nusselt number was applicable with the Notter-Rouse correlation.

Several values including the heat capacitance, thermal conductivity, density and dynamic viscosity of pure water as the base fluid were determined through the correlations recommended by Yadav *et al.*, (2016). These correlations are valid for: $278 \leq T\,(K) \leq 363$.

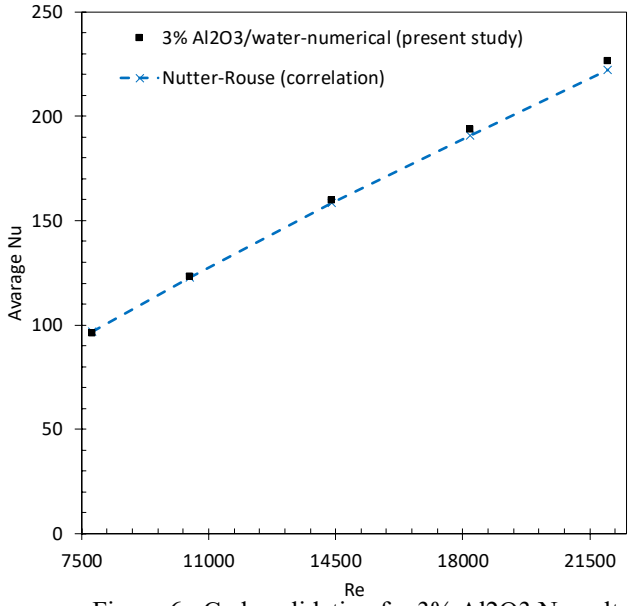

Figure 6: Code validation for 3% Al2O3 Nusselt number

3.2 Water-Ethylene and Al2O3-TiO2 HyNf properties

Evaluations of the thermal properties models, Equations (1)-(4) and validation was conducted by a comparison of ASHRAE for a mixture of EG and water in a ratio of 30:70 with the present data. The validation results are shown in Figure 7 and Figure 9 below. The results had an error of less than 0.16% for the measurement of the thermal conductivity under the MATLAB curve fitting tool. Deviation of the measured data compared to ASHRAE was negligible. Likewise, Hamid *et al.*, (2018) carried out the validation test and the error analyses compared to that of ASHRAE was up to 2%. Additionally, similar temperature range and the ratio for the mixture of water and EG were taken into consideration as was in Bahrami *et al.*, (2016) and Redhwan *et al.*, (2016). Figure 7 show results of the thermal conductivity and viscosity respectively, which indicates good comparisons with ASHRAE (1979).

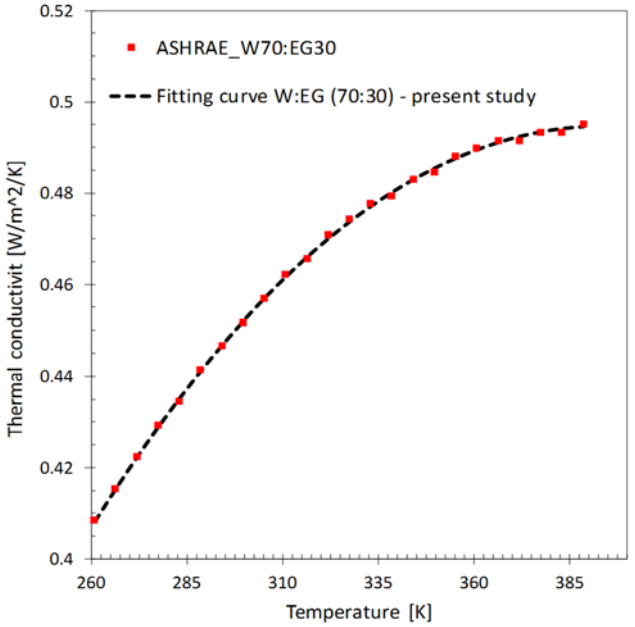

(a)

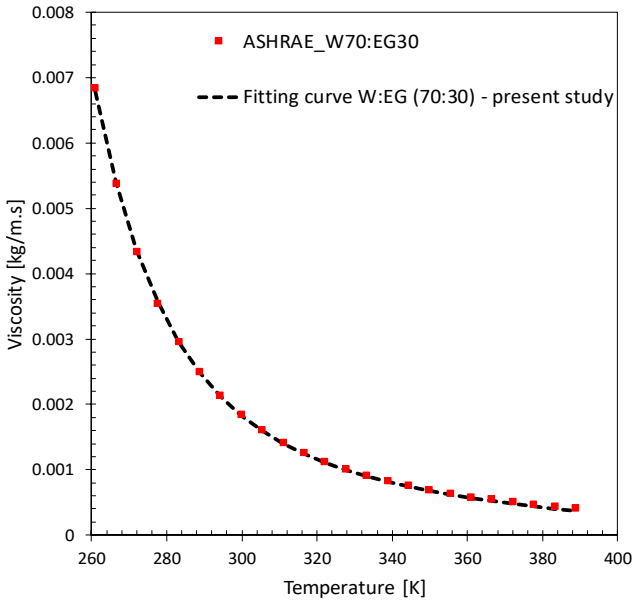

(b)

Figure 7: Validation of (a) thermal conductivity and (b) viscosity models

The viscosity and thermal conductivity of the Al_2O_3-TiO_2 HyNf at 2.5% - 1.5% and 5.0% - 3.0% volume concentrations with varied temperatures between 291K and 394K are shown below in Figure 9. From Figure 9 (a) it can be observed that the thermal conductivity of the nanofluids in question is enhanced with a rise in temperature and volume concentration. The highest result of this enhancement was identified at a volume concentration of 5.0 - 3.0% and a temperature of 394 K. Compared to the base fluids, the thermal conductivity rose up to 0.613. For all volume concentrations, the thermal conductivity the base fluid is always lower than Al_2O_3-TiO_2 HyNf. The same pattern was also spotted by former researchers such as Suresh *et al.*, (2011). Meanwhile, the viscosity of the nanofluids in question increased with increase and decrease in volume concentrations and temperature respectively, a result that aligned with the trend with which the base fluid identified as shown in Figure 9 (b) and (c). In contrast, the heat capacity of the HyNf in question increased and decreased with increasing temperature and decreasing volume concentrations respectively as illustrated in Figure 9 (d).

Illustrated graphically in Figure 8, the enhancement of the thermal conductivity of HyNf increased by 24% for 5% - 3% Al_2O_3-TiO_2 and 11.5% for 2.5%–1.5% Al_2O_3-TiO_2. In the same breath, the viscosity enhancement rose to 67% and 70% for 2.5% – 1.5% and 5% - 3% of the Al_2O_3-TiO_2 HyNf respectively. Whereas Esfe *et al.*, (2015) study, the relative thermal conductivity was 1.43 for 2% volume concentration of Cu/TiO_2 suspended in water-ethylene glycol (60:40) at 335.25 K.

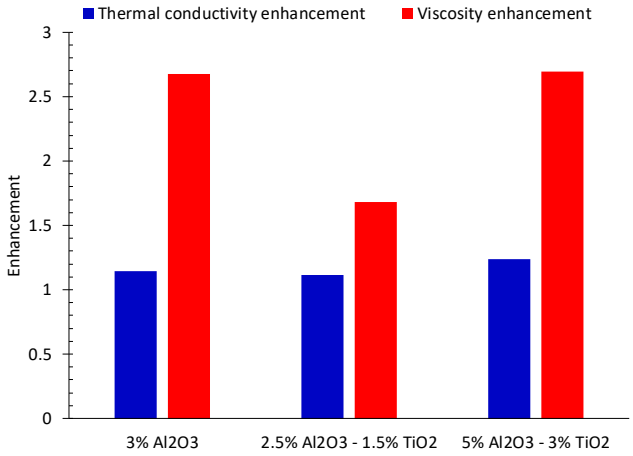

Figure 8: The enhancement of thermal conductivity and viscosity

* Corresponding author. Madeleine L Combrinck Tel.: +44 0191 299 4549; e-mail: madeleine.combrinck@northumbria.ac.uk

Figure 9

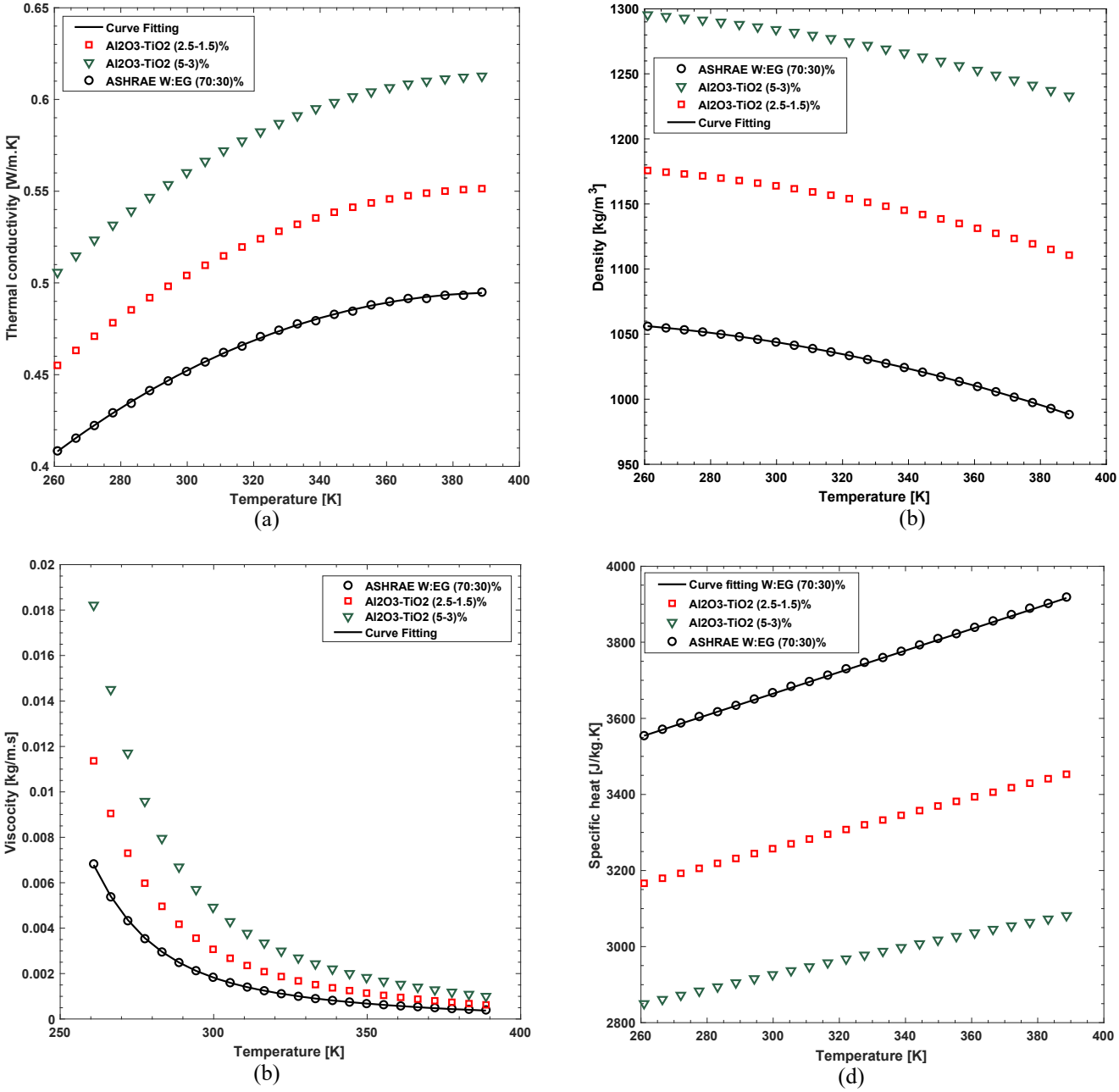

Figure 9: Thermal properties of HyNf as a function of temperature (a) Thermal Conductivity, (b)Viscosity, (c) Density and (d) Specific Heat.

3.3 Heat Transfer Analysis

A comparison of numerical results of the Nu and friction factor of the HyNf with the correlations for different Reynolds number (7800-22000) was carried out. These included Dittus and Boelter (1930), Petukhov (1970) and Notter-Rouse (1972). Further, another friction factor, the Darcy friction factor was also compared with correlation as per the suggestions of Petukhov (1970) and Blasius (1908). In regard to the calculation of the friction factor for pure fluid, the latter proposed the relation as follows:

$$f = \frac{0.316}{Re^{0.25}}, 3000 \leq Re \leq 10^5 \quad (26)$$

Petukhov equation:

$$\overline{Nu} = \frac{\frac{f}{8} RePr}{1.07 + 12.7\left(\frac{f}{8}\right)^{0.5}\left(Pr^{\frac{2}{3}} - 1\right)} \quad (27)$$

$$f = (1.82\, log\, Re - 1.64)^{-2} \quad (28)$$

Dittus and Boelter equation:

$$Nu = 0.024 Re^{0.8} Pr^{0.4} \quad (29)$$

In Figure 10, the ratio of the convection heat transfer coefficient $h_r = h_{nf}/h_f$ of HyNf to that of W:EG varies from 1.21 to 1.225 times for 2.5-1.5% concentration and further from 1.49 to 1.52 times for 5-3% concentration. However, the coefficient ratio of heat transfer for 3% Al_2O_3 varies slightly from 1.51 to 1.55 under a similar Re number. Even so, Al_2O_3-water with a concentration of 3% display better enhancement than the HyNf. This is partly because the thermal conductivity of pure EG is lower than that of pure water as outlined in Table 1.

Figure 11 and Figure 12 show the heat transfer coefficient and Nu of Al_2O_3-TiO_2 HyNf at different Re. The numerical Nu for HyNf is seen to be in agreement with the trend provided by Dittus and Boelter (1930). In addition, the base fluid made up of W:EG aligns with the Petukhov correlation of heat transfer. On the other hand, the correlation of heat transfer by Notter and Rouse somewhat underestimates the coefficient and Nu for the base fluid as in Figure 11 (a) and Figure 12 (a) as well as the HyNf as shown in Figure 11 (b) and (c) Figure 12 (b) and (c). Likewise, the results posted by Hamid *et al.*, (2018) demonstrated an agreement with the Dittus and Boelter (1930) equation outlined above.

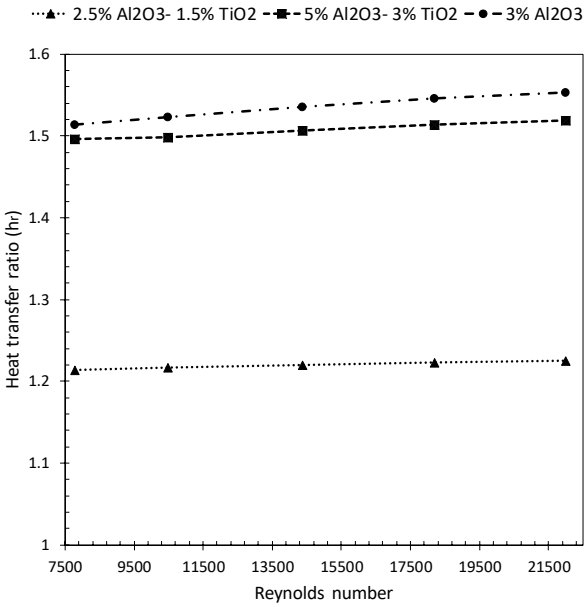

Figure 10 Heat transfer ratio for different nanofluids

As shown in Figure 13 (a), as the Re number increases, the Nusselt number also increases. It can also be seen that at certain Re number, the Nusselt number of the different volume concentrations of Al_2O_3-TiO_2 are prominently higher than the base fluid, in this case water and water and EG. This rise can be explained by the link between the nanofluids and nanoparticle. More specifically, suspended nanoparticles enhance the thermal conductivity of the mixture. Alternatively, as suggested by Xuan and Roetzel (2000) , the enhancement can be due to the sizeable energy exchange process that follows the chaotic movement of the available nanoparticles. The same increase was observed for heat transfer coefficient as shown in Figure 13 (b). The average heat transfer coefficient increase is high and even much higher for 5% Al_2O_3 and 3% TiO_2. For this reason, as expected, Nano fluids identify with higher thermal capability that their counterpart, the base fluid. It is also noteworthy that the convective heat transfer between the fluid and the wall should be more efficient with higher thermal conductivity of the HyNf. One interesting finding is that the heat transfer coefficient for water was lower than W:EG even though water has higher thermal conductivity. Thus, the heat transfer enhancement does not only depend on thermal conductivity but also depends on other properties.

* Corresponding author. Madeleine L Combrinck Tel.: +44 0191 299 4549; e-mail: madeleine.combrinck@northumbria.ac.uk

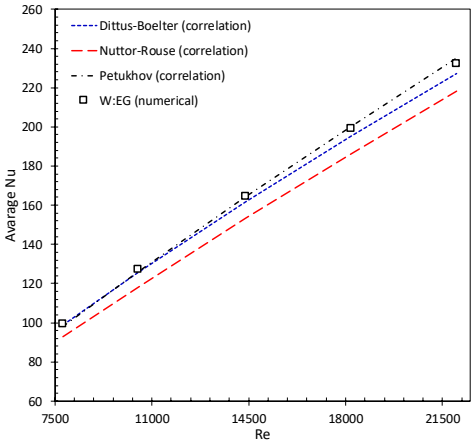

(a) Water-Etheylene glycol (70:30)

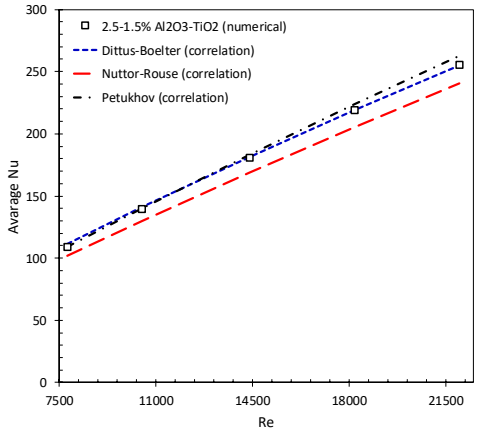

(b) 2.5-1.5 % Al2O3-TiO2

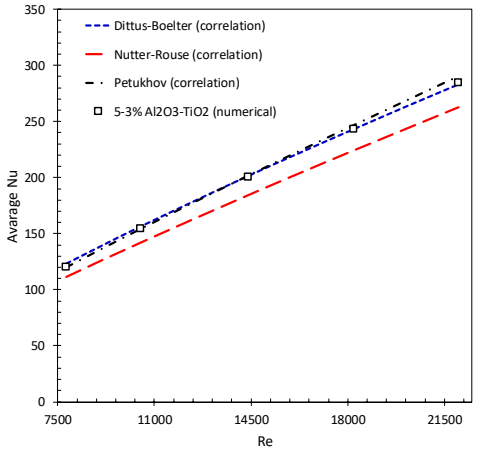

(c) 5-3 % Al2O3-TiO2

Figure 11: Comparasion between numerical Nu and available Nu correlations

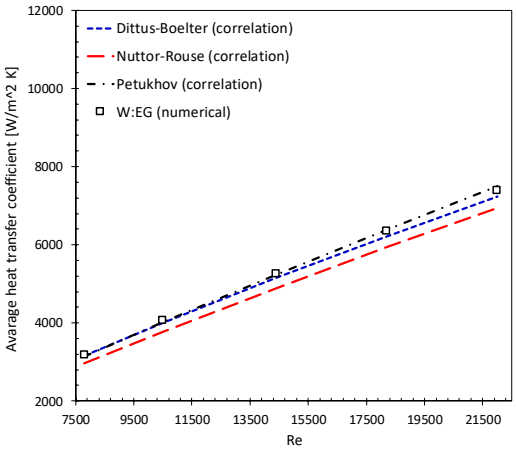

(a) Water-Etheylene glycol (70:30)

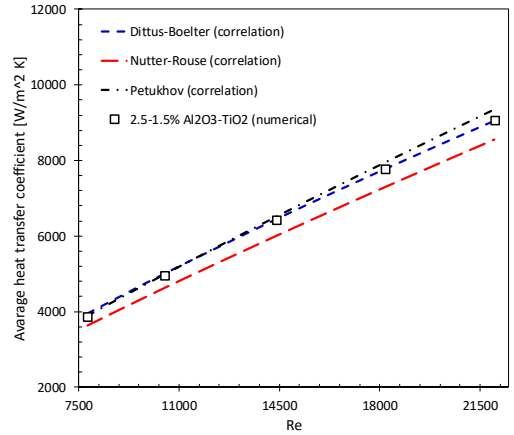

(b) 2.5-1.5 % Al2O3-TiO2

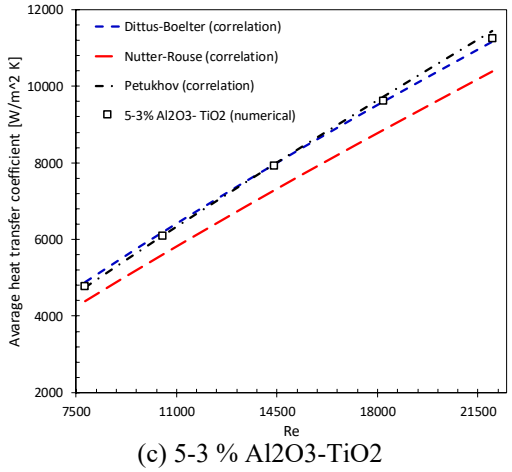

(c) 5-3 % Al2O3-TiO2

Figure 12 Comparasion between numerical $\bar{h}$ and analytical $\bar{h}$

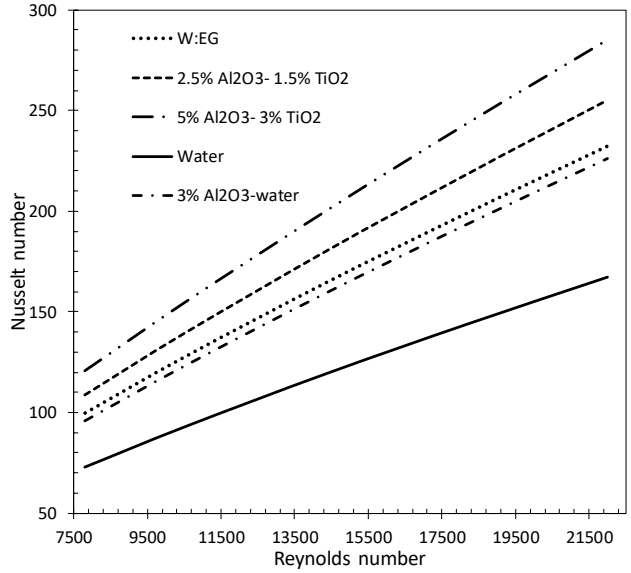

(a)

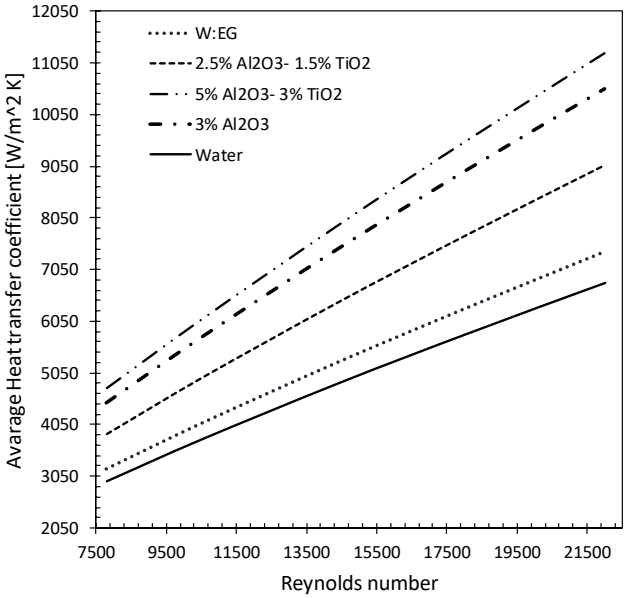

(b)

Figure 13 Numerical average (a)Nusselt number and (b) heat transfer coefficient

3.4 Pressure Drop and Friction Factor

When the practical application of HyNf or even nanofluid alone is considered, it is important to study and observe the pressure, whether it is dropped or developed as the coolants flow. For this reason, the impact of the HyNf and nanofluid in this case on the friction factor was observed at different Re number and volume concentrations visible on Figure 14-17. The viscosity and density of the base fluid increased following an increase in the amount of nanoparticles loaded into the base fluid. This resulted a pressure drop and the creation of a higher friction factor.

Figure 14 presents the friction factor of HyNf (Al2O3-TiO2) and their base fluid. The numerical results for the W:EG (70:30) mixture were compared with Blasius (1943) and Petukhov (1970) given by equation (26) and (28). The results of this comparison fell between the two lines Blasius and Petukhov. On the contrary, Hamid *et al.*, (2018) found that the correlation developed by Blasius was in agreement with the result for a W:EG base fluid on a 60:40 ratio. Figure 15 also points to the finding that the friction factor of the HyNf is higher than that of the base fluids, albeit slightly, especially at Reynolds number 7800 and insignificant at other Re. Moreover, 3% Al2O3-water displays same result as Al2O3-TiO2 with concentration of 5-3%. Further, the distribution of the friction factor stayed near the Blasius line for all the concentration and reduced exponentially as the Re number increased as illustrated in Figure 14 (a) and Figure 14 (b). Therefore, the nanofluids in question have the potential of affecting the friction factor to achieve higher particle volume concentration. Similar findings were also posted by Redhwan *et al.*, (2017), Pak and Cho, (1998) and Bozorgan (2012). The viscosity of HyNf diminished as the temperature increased. This might lead to a small drop in the measured pressure of the HyNf. As outlined in Table 3, Al2O3-TiO2 with concentration of 5-3% may need extra pumping power as a result of the high viscosity.

Table 3 Thermophysical properties for base fluids and nanofluids at T 293 K

	k [W/mK]	**μ** [kg/ms]	**ρ** [kg/m³]	**C_p** [J/kgK]	**T_B** [K]	**T_F** [K]
Water	0.613	0.001	996.5	4181	373.15	273.15
W:EG (70:30)	0.252	0.0157	1111.4	2415	377.59	259.1
3% Al_2O_3-water	0.6525	0.0027	1085.6	3776.9	-	-
2.5% Al_2O_3-1.5% TiO_2	0.4969	0.0037	1166.6	3241.5	-	-
5% Al_2O_3-3% TiO_2	0.5524	0.0059	1286.6	2913.3	-	-

* Corresponding author. Madeleine L Combrinck Tel.: +44 0191 299 4549; e-mail: madeleine.combrinck@northumbria.ac.uk

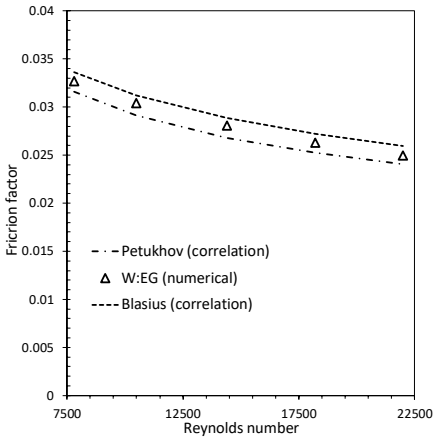

(a)

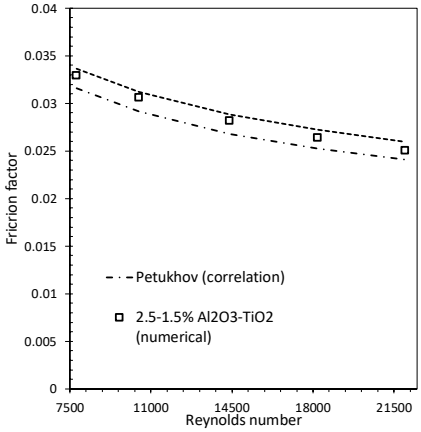

(b)

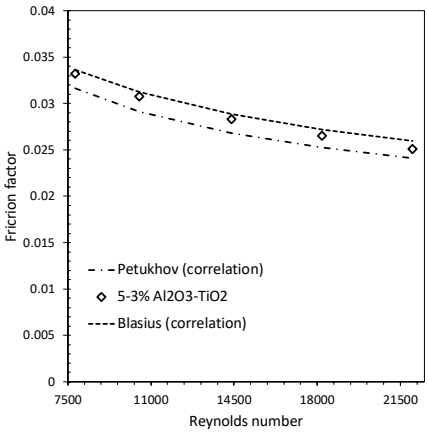

(c)

Figure 14 Comapring Petukhov and Blasius friction factor correlatios with (a) W:EG , (b) 2.5-1.5% Al2O3-TiO2 and (c) 5-3% Al2O3-TiO2

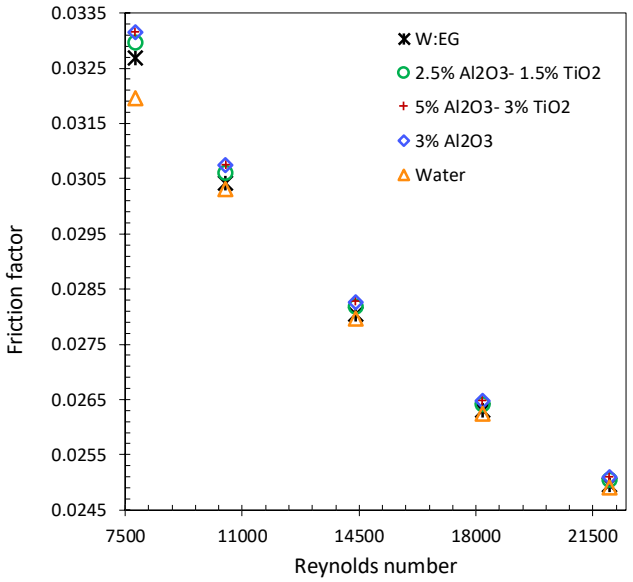

Figure 15 Friction factor of HyNf, nanofluid and their base fluid comparision at various Re

3.5 Bulk and wall temperature profiles

Figure 16 illustrates wall and bulk temperature profiles along tube axis for Re 22000. Noticeably, the decline of bulk and wall temperatures for HyNf and nanofluid, with regard to the base fluid, rises with the x axis. For a concentration of 3% of Al2O3, wall and bulk temperatures are lower than water while a HyNf (Al2O3-TiO2) with concentration 2.5-1.5%, the wall and bulk temperatures are higher than Al2O3-TiO2 with concentration of 5-3% and lower than the base fluid (W:EG). These findings indicate the positive impact as a result of nanoparticles, which are explicable by the fact that their presence has led to significant improvement on the thermal properties of the mixture. Additionally, the difference between wall and bulk temperature is lowered against the base fluid, thereby triggering increased heat transfer.

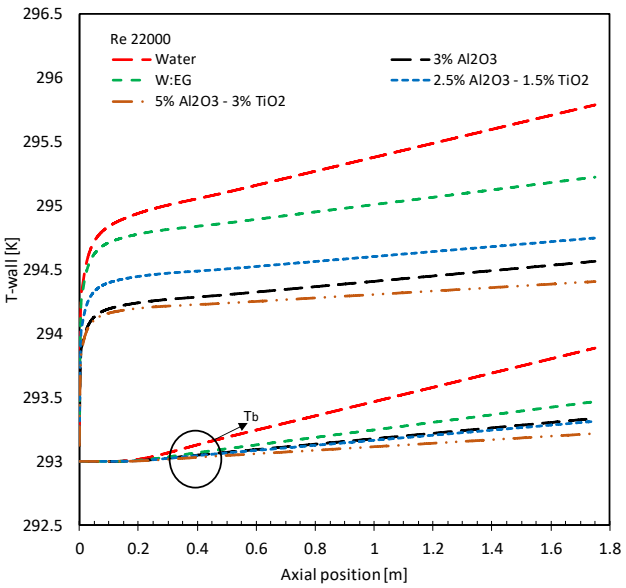

Figure 16 The axial wall and bulk developed temperature

Figure 17 shows radial temperatures at x/D = 125 for Reynolds number 22000 that are investigated. Temperature in this case, for the most part, depends on volume concentration. This is to mean that when the volume concentration increase, the fluid temperature is reduced. This is mostly the case near the tube wall. In addition, the difference that exists between temperature values for both the HyNf and the base fluid increases simultaneously as the radial position. This points to the achievement of a higher heat transfer rate with nanoparticles. For the HyNf that identify with a concentration of 5 - 3% identify with lower temperatures that are lower than concentrations of 2.5-1.5% as well as the temperatures of the base fluid (W:EG). This trend is also observable for 3% Al_2O_3 and the water base fluid at a radial position that is less than 0.0065m. Further, the difference between the temperature at the surface (x = 0.007) and that at the axis (x = 0) is lowest for Al_2O_3-TiO_2 at 5 - 3%. When the concentration of the HyNf stands at 2.5 - 1.5%, the temperature difference is decreased for 3% Al_2O_3 / water.

However, these findings are not enough to explain the increase in the heat transfer as a result of nanofluids. This is due to the fact that increase in heat transfer is typically higher than the increase in thermophysical properties. Several authors, seeking to explain these effects, have come with different explanations and suggestions. For instance, Buongiorno (2006) posed the suggestion that an increase in the heat transfer coefficient results when the Prandtl number examined with bulk properties (Pr_{bulk}) is higher or greater than that which is examined with laminar sub-layer properties ($Pr_{sub\text{-}layer}$). In as far the Prandtl theory is concerned, evaluation of the Nusselt number numerator is done at Pr_{bulk} while the denominator is evaluated at $Pr_{sub\text{-}layer}$. The behaviour exhibited by both $Pr_{sub\text{-}layer}$ and Pr_{bulk} chiefly depends on a viscosity at the laminar sub-layer that is lower than that the bulk, while the thermal conductivity at the laminar sub-layer is larger than that at the bulk. This impact is also observable in pure liquids. This effect is also present in pure liquids. However, according to Buongiorno (2006) it is more pronounced for nanofluids since the nanofluid viscosity strongly depends on the temperature and because of the conductivity present in the laminar sub-layer.

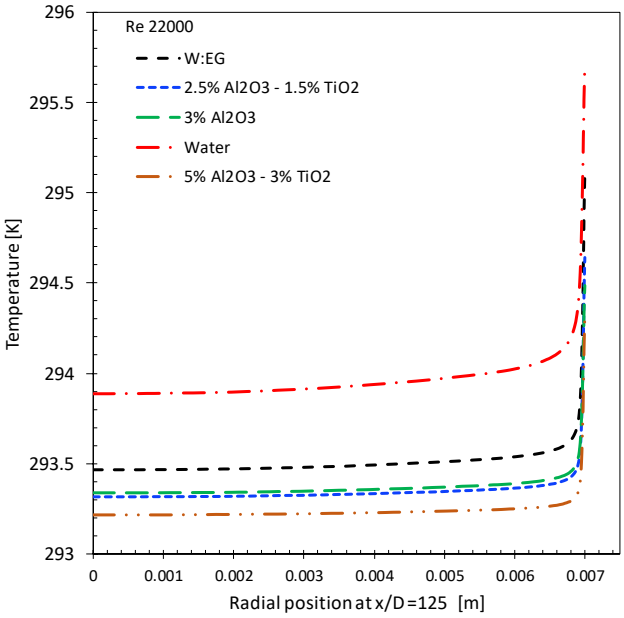

Figure 17 Temperature profile for Re 22000 at x/D=125

3.6 Average Shear Stress Ratio

Figure 18 below showcases the impact of various nanoparticle volume concentrations of Al2O3/water and Al2O3-TiO2/W:EG nanofluids on the average shear stress ratio, $\bar{\tau}_r = \bar{\tau}_{nf}/\bar{\tau}_f$. This investigation found that the average shear stress ration increases as the volume of the nanoparticle increases. This enhancement is chiefly independent on the Re number. For instance, for Re = 14400 HyNf, the value of $\bar{\tau}$ is 2.53 for a volume particles concentration of 2.5-1.5%. In addition, for a higher particle volume concentration such as that of 5-3% particles, the value of $\bar{\tau}$ is 5.92. The higher results have also been

* Corresponding author. Madeleine L Combrinck Tel.: +44 0191 299 4549; e-mail: madeleine.combrinck@northumbria.ac.uk

returned for the 3% Al_2O_3, which returned a $\bar{\tau}_r$value of 6.54. From these findings, it can be concluded that a rise in the average shear stress ratio as regards the nanoparticle volume concentration is significant for both nanofluids (i.e. HyNf and nanofluid). This increase of the average sheer stress ratio can be attributed to the effects of rise in pressure or frictional force.

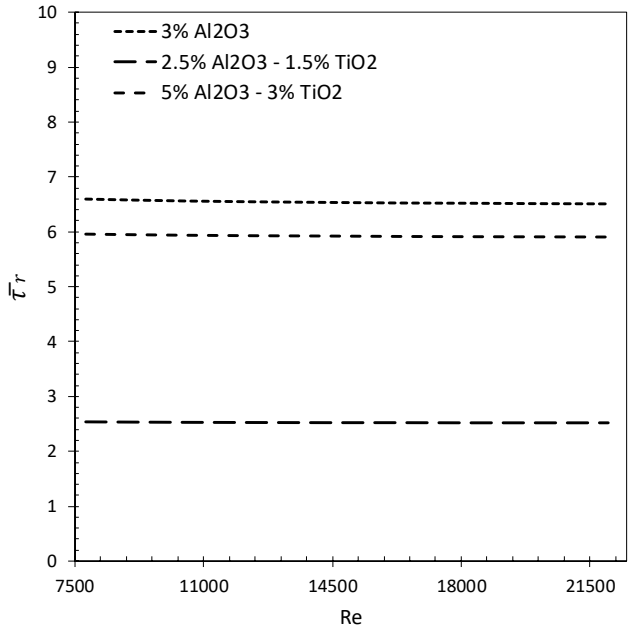

Figure 18 Avarage shear stress coefficient ratio of nanofluids at varied Re

3.7 Thermal performance factor

Revelations from the numerical investigation carried out for the friction factor and heat transfer performance show that a noticeable rise in the thermal conductivity as well as that of the heat transfer coefficient can be attained by factoring in low concentration of nanoparticles in conventional heat transfer fluids. This results in a better heat transfer performance of the associated thermal systems. In the same breath, enhancement in the heat transfer performance with nanofluids is typically followed by an increase in their viscosity as well as a reduction in pressure. As a result, seeing that these effects are not the most desirable, it limits the application of nanofluids. Hemmat *et al.*, (2013) assert that there is need for identifying the optimum operating conditions to lift these limitations in practical application of nanofluids. The thermal performance factor is often used in heat transfer systems for the purposes of finding optimum conditions. It is understood as the ratio between the Nu ratio and the friction factor ratio as provided by equation (30) (Suresh, Chandrasekar and Selvakumar, 2012).

$$Performance\ factor = \frac{(Nu_{nf}/Nu_f)}{\sqrt[3]{(f_{nf}/f_f)}} \quad (30)$$

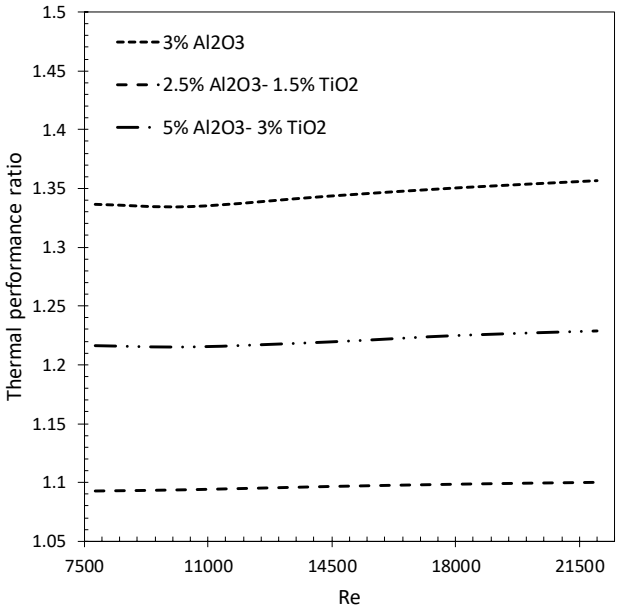

Figure 19 Variation of thermal performance factor with Reynolds number

Figure 19 showcases the thermal performance factor discussed above. The factor is investigated using various volume concentrations of 3% Al_2O_3/water as well as 5-3% and 2.5-1.5% Al_2O_3-TiO_2/W:EG. Observations point to the fact that the value of thermal performance factor manages to stay greater than one for all volume concentrations included in the investigation. This thermal performance factor also stays close to the ratio of the average heat transfer of nanofluids to the base fluid. Additionally, the ratio of Darcy friction factor observed as regards the nanofluids to base fluid is close to one.

Thus, it can be concluded that it is possible to enhance heat transfer regardless of whether there is little or zero penalty in the pumping power. In practical application, this can lead to greater efficiency and even reduced costs of energy. It is also observable from the investigation that the thermal performance ratio increases when the nanoparticle volume concentration increases for different concentrations of nanofluids. Alternatively, it may be due to the fact that both thermal conductivity of nanofluids and dynamic viscosity increase when nanoparticle volume concentration is

increased. Therefore, increased viscosity leads to a reduction of the thickness of the boundary layer, which then results in enhanced heat transfer while higher thermal conductivity informs enhancement of the thermal performance factor.

6. Conclusion

In this numerical study, the thermal properties and heat transfer characteristics of hybrid nanoparticles Al2O3-TiO2 suspended in a water-ethylene glycol (70:30) mixture has been examined for two concentrations 2.5-1.5% and 5-3% using a circular pipe geometry under turbulent conditions. The HyNf simulations have been run under varied Reynolds number from 7800 to 22000 at constant heat flux, and the inlet temperature was 293 K. The maximum enhancement during simulations for thermal conductivity was 24% and 11% when the concentrations of nanoparticles stand at 5-3% and 2.5-1.5%, respectively. Whereas, dynamic viscosity rose up by 67% and 70% for 2.5-1.5% and 5-3% volume concentration of HyNf, respectively.

The investigation of heat transfer has shown that the Dittus and Boelter correlation for Nusselt number was in a good agreement with numerical result. Also, the heat transer coefficient generally increased as Rynolds number and the volume concentration increased which lead to enhance thermal conductivity. Heat transfer of HyNf were enhanced by 22.5% and 52% for 2.5-1.5% and 5-3% volume concentration, respectively, at Re 22000 for a double based mixture water-ethylene glycol fluid. The enhancement in heat transfer for 3% Al2O3-water base fluid was higher than HyNf due to water base fluid having a higher thermal conductivity than water-ethylene glycol base fluid.

One of the findings to emerge from this study is that Blasius correlation for friction factor showed higher accurcy in perdicting numerical friction factor than Petkhove correlation. It was noted that the friction factor inreased due to the paticles loaded in the base fluid and decrased by increasing Reynoalds number. Al2O3-TiO2 HyNf with concentrations of 5-3% respectively exhibited the highest friction factor due to its higher viscosity. This might lead to a pressure drop which may require additonal extra pumping power. Once the viscosity is decreased by increasing temperature, this formulation for a HyNf under high working temperature to overcome the pressure dorp.

These finding suggest a role for Al2O3-TiO2 nanoparticles dispersed into W:EG in applications where enhanced heat transfer is required.

7. References

Akilu, S. *et al.* (2016) 'A review of thermophysical properties of water based composite nanofluids', *Renewable and Sustainable Energy Reviews*, 66, pp. 654–678. doi: https://doi.org/10.1016/j.rser.2016.08.036.

ASHRAE (1979) *American society of heating, refrigerating and air-conditioning engineers*, *International Journal of Refrigeration*. doi: 10.1016/0140-7007(79)90114-2.

Baghbanzadeh, M. *et al.* (2014) 'Investigating the rheological properties of nanofluids of water/hybrid nanostructure of spherical silica/MWCNT', *Thermochimica Acta*, 578, pp. 53–58. doi: https://doi.org/10.1016/j.tca.2014.01.004.

Bahrami, M. *et al.* (2016) 'An experimental study on rheological behavior of hybrid nanofluids made of iron and copper oxide in a binary mixture of water and ethylene glycol: Non-Newtonian behavior', *Experimental Thermal and Fluid Science*, 79, pp. 231–237. doi: https://doi.org/10.1016/j.expthermflusci.2016.07.015.

Batchelor, G. K. (1977) 'Effect of Brownian-motion on Bulk Stress in a Suspension of Spherical-particles', *Journal of Fluid Mechanics*. 2006/04/12. Cambridge University Press, 83(NOV), pp. 97–117. doi: 10.1017/S0022112077001062.

Bianco, V., Manca, O. and Nardini, S. (2011) 'Numerical investigation on nanofluids turbulent convection heat transfer inside a circular tube', *International Journal of Thermal Sciences*. Elsevier Masson SAS, 50(3), pp. 341–349. doi: 10.1016/j.ijthermalsci.2010.03.008.

Blasius, H. (1943) 'National advisory committee for aeronautics', *Journal of Applied Physics*, 14(8), pp. 399–405. doi: 10.1063/1.1715007.

Bozorgan, N. (2012) 'Evaluation of Using Al 2 O 3 / EG and TiO 2 / EG Nanofluids as Coolants in the Double-tube Heat Exchanger', 5(2).

Brailsford, A. D. and Major, K. G. (1964) 'The thermal conductivity of aggregates of several phases, including porous materials', *British Journal of Applied Physics*, 15(3), pp. 313–319. doi: 10.1088/0508-3443/15/3/311.

Buongiorno, J. (2006) 'Convective Transport in Nanofluids', *Journal of Heat Transfer*, 128(3), p. 240. doi: 10.1115/1.2150834.

Che Sidik, N. A. *et al.* (2017) 'A review on preparation methods, stability and applications of hybrid nanofluids', *Renewable and Sustainable Energy Reviews*, 80, pp. 1112–1122. doi: https://doi.org/10.1016/j.rser.2017.05.221.

Choi, U. S. (1995) 'Enhancing thermal conductivity of fluids with nano-particles', *ASME, FED*, 231, pp. 99–105. Available at:

* Corresponding author. Madeleine L Combrinck Tel.: +44 0191 299 4549; e-mail: madeleine.combrinck@northumbria.ac.uk

http://ci.nii.ac.jp/naid/80008813348/en/ (Accessed: 1 September 2018).

Deepak Selvakumar, R. and Dhinakaran, S. (2016) 'Nanofluid flow and heat transfer around a circular cylinder: A study on effects of uncertainties in effective properties', *Journal of Molecular Liquids*, 223, pp. 572–588. doi: https://doi.org/10.1016/j.molliq.2016.08.047.

Dittus, F. W. and Boelter, L. M. K. (1930) 'Heat transfer in automobile radiator of the tube type', *University of California, Publication in Engineering*, 2, p. 443. Available at: http://www.sciencedirect.com/science/article/B6V3F-497B9NS-H/2/119fb9d6bf5237677d991e2083411241.

Ebrahimi, S. *et al.* (2010) *New Class of Coolants: Nanofluids*. Available at: www.intechopen.com.

Esfe, M. *et al.* (2015) 'Thermal conductivity of Cu/TiO<inf>2</inf>-water/EG hybrid nanofluid: Experimental data and modeling using artificial neural network and correlation', *International Communications in Heat and Mass Transfer*, 66, pp. 100–104. doi: 10.1016/j.icheatmasstransfer.2015.05.014.

FAN, S., LAKSHMINARAYANA, B. and BARNETT, M. (1993) 'Low-Reynolds-number k-epsilon model for unsteady turbulent boundary-layer flows', *AIAA Journal*. American Institute of Aeronautics and Astronautics, 31(10), pp. 1777–1784. doi: 10.2514/3.11849.

Hamid, K. A. *et al.* (2018) 'Experimental investigation of thermal conductivity and dynamic viscosity on nanoparticle mixture ratios of TiO2-SiO2nanofluids', *International Journal of Heat and Mass Transfer*. Elsevier Ltd, 116, pp. 1143–1152. doi: 10.1016/j.ijheatmasstransfer.2017.09.087.

Hamzah, M. H. *et al.* (2017) 'Factors affecting the performance of hybrid nanofluids: A comprehensive review', *International Journal of Heat and Mass Transfer*, 115, pp. 630–646. doi: https://doi.org/10.1016/j.ijheatmasstransfer.2017.07.021.

Hemmat Esfe, M. *et al.* (2015) 'Experimental determination of thermal conductivity and dynamic viscosity of Ag–MgO/water hybrid nanofluid', *International Communications in Heat and Mass Transfer*, 66, pp. 189–195. doi: https://doi.org/10.1016/j.icheatmasstransfer.2015.06.003.

Hemmat, M. *et al.* (2013) 'Experimental studies on the convective heat transfer performance and thermophysical properties of MgO-Water nanofluid under turbulent flow', *Exp. Therm. Fluid. Sci.*, 52, pp. 68–78. doi: 10.1016/j.expthermflusci.2013.08.023.

Ho, C. J. *et al.* (2010) 'Preparation and properties of hybrid water-based suspension of Al 2O 3 nanoparticles and MEPCM particles as functional forced convection fluid', *International Communications in Heat and Mass Transfer*, 37(5), pp. 490–494. doi: 10.1016/j.icheatmasstransfer.2009.12.007.

Ho, C. J., Chen, W.-C. and Yan, W.-M. (2014) 'Experiment on thermal performance of water-based suspensions of Al 2O3 nanoparticles and MEPCM particles in a minichannel heat sink', *International Journal of Heat and Mass Transfer*, 69, pp. 276–284. doi: 10.1016/j.ijheatmasstransfer.2013.10.034.

Hussein, A. M. (2017) 'Thermal performance and thermal properties of hybrid nanofluid laminar flow in a double pipe heat exchanger', *Experimental Thermal and Fluid Science*. Elsevier Inc., 88, pp. 37–45. doi: 10.1016/j.expthermflusci.2017.05.015.

Kakaç, S. and Pramuanjaroenkij, A. (2016) 'Single-phase and two-phase treatments of convective heat transfer enhancement with nanofluids - A state-of-the-art review', *International Journal of Thermal Sciences*, 100, pp. 75–97. doi: 10.1016/j.ijthermalsci.2015.09.021.

Kumar, N. and Sonawane, S. S. (2016) 'Experimental study of Fe2O3/water and Fe2O3/ethylene glycol nanofluid heat transfer enhancement in a shell and tube heat exchanger', *International Communications in Heat and Mass Transfer*, 78, pp. 277–284. doi: https://doi.org/10.1016/j.icheatmasstransfer.2016.09.009.

Launder B.E. and Sharama (1974) 'Application of the energy dissipation model of turbulence to the calculation of flow near a spining disc', *letters in Heat and Mass Transfer*, 1(2), p. 1974.

Li, Q. and Xuan, Y. (2000) 'Heat Transfer Enhancement of Nanofluids', *International Journal of Heat and Mass Transfer*, 21(1), pp. 58–64.

Madhesh, D. and Kalaiselvam, S. (2014) 'Experimental Analysis of Hybrid Nanofluid as a Coolant', *Procedia Engineering*, 97, pp. 1667–1675. doi: https://doi.org/10.1016/j.proeng.2014.12.317.

Madhesh, D., Parameshwaran, R. and Kalaiselvam, S. (2014) 'Experimental investigation on convective heat transfer and rheological characteristics of Cu-TiO2 hybrid nanofluids', *Experimental Thermal and Fluid Science*, 52, pp. 104–115. doi: 10.1016/j.expthermflusci.2013.08.026.

Masuda, H. *et al.* (1993) 'Alteration of Thermal Conductivity and Viscosity of Liquid by Dispersing Ultra-Fine Particles. Dispersion of Al2O3, SiO2 and TiO2 Ultra-Fine Particles.', *Netsu Bussei*, 7(4), pp. 227–233. doi: 10.2963/jjtp.7.227.

Minea, A. A. (2017a) 'Challenges in hybrid nanofluids behavior in turbulent flow: Recent research and numerical comparison', *Renewable and Sustainable Energy Reviews*. doi: 10.1016/j.rser.2016.12.072.

Minea, A. A. (2017b) 'Hybrid nanofluids based on Al2O3, TiO2and SiO2: Numerical evaluation of different approaches', *International Journal of Heat and Mass Transfer*, 104, pp. 852–860. doi: 10.1016/j.ijheatmasstransfer.2016.09.012.

Moghadassi, A., Ghomi, E. and Parvizian, F. (2015) 'A numerical study of water based Al2O3 and Al2O3-Cu hybrid nanofluid effect on forced convective heat transfer', *International Journal of Thermal Sciences*, 92, pp. 50–57. doi: 10.1016/j.ijthermalsci.2015.01.025.

Notter, R. H. and Sleicher, C. A. (1972) *A solution to the turbulent Graetz problem-III Fully developed and entry region heat transfer rates*, *Chemical Engineering Science*. doi: 10.1016/0009-2509(72)87065-9.

Nuim Labib, M. *et al.* (2013) 'Numerical investigation on effect of base fluids and hybrid nanofluid in forced convective heat transfer', *International Journal of Thermal Sciences*. Elsevier Masson SAS, 71, pp. 163–171. doi: 10.1016/j.ijthermalsci.2013.04.003.

Pak, B. C. and Cho, Y. I. (1998) 'Hydrodynamic and heat transfer study of dispersed fluids with submicron metallic oxide particles', *Experimental Heat Transfer*. Taylor & Francis, 11(2), pp. 151–170. doi: 10.1080/08916159808946559.

Petukhov, B. S. (1970) 'Heat Transfer and Friction in Turbulent Pipe Flow with Variable Physical Properties', *Advances in Heat Transfer*, 6, pp. 503–564. doi: 10.1016/S0065-2717(08)70153-9.

Redhwan, A. A. M. *et al.* (2016) '01.Development of nanorefrigerants for various types of refrigerant based : A comprehensive review on performance ☆', *International Communications in Heat andMass Transfer*, 76, pp. 285–293. doi: https://doi.org/10.1016/j.icheatmasstransfer.2016.06.007.

Redhwan, A. A. M. *et al.* (2017) 'Comparative study of thermo-physical properties of SiO2 and Al2O3 nanoparticles dispersed in PAG lubricant', *Applied Thermal Engineering*, 116, pp. 823–832. doi: https://doi.org/10.1016/j.applthermaleng.2017.01.108.

Saha, G. and Paul, M. C. (2014a) 'Numerical analysis of the heat transfer behaviour of water based Al2O3and TiO2nanofluids in a circular pipe under the turbulent flow condition', *International Communications in Heat and Mass Transfer*, 56(C), pp. 96–108. doi: 10.1016/j.icheatmasstransfer.2014.06.008.

Saha, G. and Paul, M. C. (2014b) 'Numerical analysis of the heat transfer behaviour of water based Al2O3and TiO2nanofluids in a circular pipe under the turbulent flow condition', *International Communications in Heat and Mass Transfer*, 56, pp. 96–108. doi: 10.1016/j.icheatmasstransfer.2014.06.008.

Sarboolookzadeh Harandi, S. *et al.* (2016) 'An experimental study on thermal conductivity of F-MWCNTs–Fe3O4/EG hybrid nanofluid: Effects of temperature and concentration', *International Communications in Heat and Mass Transfer*, 76, pp. 171–177. doi: https://doi.org/10.1016/j.icheatmasstransfer.2016.05.029.

Schildknecht, M., Miller, J. A. and Meier, G. E. A. (1979) 'The influence of suction on the structure of turbulence in fully developed pipe flow', *Journal of Fluid Mechanics*, 90(1), pp. 67–107. doi: 10.1017/S0022112079002081.

Shih, T. H. *et al.* (1995) *A new k-ε turbulent eddy viscosity model for high reynolds number turbulent flows*, *Computers and Fluids*. Edited by U. S. N. A. and S. Administration. [Washington, DC] : [Springfield, Va: National Aeronautics and Space Administration ; National Technical Information Service, distributor (NASA technical memorandum ; 106721.). doi: 10.1016/0045-7930(94)00032-T.

Sundar, L. S., Singh, M. K. and Sousa, A. C. M. (2014) 'Enhanced heat transfer and friction factor of MWCNT-Fe3O4/water hybrid nanofluids', *International Communications in Heat and Mass Transfer*. doi: 10.1016/j.icheatmasstransfer.2014.01.012.

Suresh, S. *et al.* (2011) 'Synthesis of Al2O3–Cu/water hybrid nanofluids using two step method and its thermo physical properties', *Colloids and Surfaces A: Physicochemical and Engineering Aspects*, 388(1), pp. 41–48. doi: https://doi.org/10.1016/j.colsurfa.2011.08.005.

Suresh, S. *et al.* (2012) 'Effect of Al2O3-Cu/water hybrid nanofluid in heat transfer', *Experimental Thermal and Fluid Science*. Elsevier Inc., 38, pp. 54–60. doi: 10.1016/j.expthermflusci.2011.11.007.

Suresh, S. *et al.* (2014) 'Turbulent heat transfer and pressure drop characteristics of dilute water based Al2O3-Cu hybrid nanofluids', *Journal of Nanoscience and Nanotechnology*, 14(3), pp. 2563–2572. doi: 10.1166/jnn.2014.8467.

Suresh, S., Chandrasekar, M. and Selvakumar, P. (2012) 'Experimental studies on heat transfer and friction factor characteristics of CuO/water nanofluid under laminar flow in a helically dimpled tube', *Heat and Mass Transfer/Waerme- und Stoffuebertragung*. Elsevier Inc., 48(4), pp. 683–694. doi: 10.1007/s00231-011-0917-2.

Takabi, B. and Shokouhmand, H. (2015) 'Effects of Al2O3–Cu/water hybrid nanofluid on heat transfer and flow characteristics in turbulent regime', *International Journal of Modern Physics C*, 26(04). doi: 10.1142/S0129183115500473.

Xuan, Y. and Roetzel, W. (2000) 'Conceptions for heat transfer correlation of nanofluids', *International Journal of Heat and Mass Transfer*, 43(19), pp. 3701–3707. doi: https://doi.org/10.1016/S0017-9310(99)00369-5.

Yadav, V. *et al.* (2016) 'Numerical investigation of heat transfer in extended surface microchannels', *International Journal of Heat and Mass Transfer*, 93, pp. 612–622. doi: https://doi.org/10.1016/j.ijheatmasstransfer.2015.10.023.

8. Nomenclature

Abbreviations

Al_2O_3	alumina
Cp	specific heat [J/Kg K]
D	pipe dimeter [m]
f	friction factor
HyNf	hybrid nanofluids
h	heat transfer [W/m^2 K]
k	thermal conductivity [W/m K]
L	pipe length [m]
Nu	Nusselt number
$\dot{m}$	Mass flow rate [m/s^2]
Pr	Prandtl number
q_s	heat flux [W/m^2]
Re	Reynolds number
r	radial coordinate [m]
T	temperature [K]
TiO2	titania
v	velocity [m/s]

* Corresponding author. Madeleine L Combrinck Tel.: +44 0191 299 4549; e-mail: madeleine.combrinck@northumbria.ac.uk

W:EG	water: ethylene glycol

Greek symbols

φ	particle volume concentration
μ	dynamic viscosity [kg/m s]
ρ	density [kg/m^3]
$\bar{\tau}$	average wall shear stress [Pa]

Subscripts

B	boiling temperature
b	bulk
eff	effective
F	freezing temperature
f	base fluid
i	inlet
m	mean
nf	nanofluid, hybrid nanofluids
w	wall
x	x direction
1	correspondence property of the 1st material
2	correspondence property of the 2nd material